Available online at www.sciencedirect.com
SCIENCE DIRECT®

Journal of the European Ceramic Society 24 (2004) 455–462

www.elsevier.com/locate/jeurceramsoc

Preparation of potassium tantalate thin films through chemical solution deposition

J. Buršík[a,*], I. Drbohlav[b], P. Vaněk[b], V. Železný[b]

[a]*Institute of Inorganic Chemistry, Academy of Sciences of the Czech Republic, 25068 Řež, Czech Republic*
[b]*Institute of Physics, Academy of Sciences of the Czech Republic, Na Slovance 2, 182 21 Prague, Czech Republic*

Abstract

Potassium tantalate (KT) $KTaO_3$ thin films of both pyrochlore and perovskite cubic structures were prepared through the chemical solution deposition (CSD). A homogeneous and stable precursor solution was obtained from potassium iso-butoxide and tantalum iso-butoxide in absolute iso-butanol with an additive of diethanolamine as a stabilizer. The effects of K:Ta sol stoichiometry, type of substrate (both amorphous, and single crystal substrates), type of buffer interlayer [Al_2O_3, Y-stabilized ZrO_2(YSZ), $PbTiO_3$, $PbTiO_3$–Al_2O_3 composite, $KNbO_3$ (KN)], and annealing regime on the kinetics of pyrochlore to perovskite transition has been studied. KT perovskite films have been successfully prepared on (100)MgO, and (0001)Al_2O_3. Using SiO_2 and Si substrates, perovskite films have been obtained via insertion of Al_2O_3 and $KNbO_3$ buffer layers.

Keywords: Chemical solution deposition; Films; Tantalates; X-ray methods

1. Introduction

Potassium tantalate niobate, $KTa_{1-x}Nb_xO_3$, thin films have received a great deal of attention thanks to its piezoelectric, pyroelectric, and electrooptic properties. The most frequently studied paraelectric cubic phase of KTN (Ta/Nb = 65/35) is a good candidate material for IR detectors and electro-optic devices thanks to its very large quadratic electrooptic coefficient and photorefractive effect.[1] Pure KT is an incipient ferroelectric with relatively high permittivity (≈230 at room temperature). It has been used in electric capacitors for DRAMs, and attracts also attention in the branch of fuel cells research owing to its high-temperature protonic conductivity.[2] Its simple cubic crystal structure and the fact that it keeps it for all temperatures (incipient ferroelectricity) make it interesting for fundamental physical study. Doping it with impurities leads to ferroelectric instability, which provides a model for induced ordering. Using different procedures including CSD method KTN perovskite thin films have been successfully prepared.[1,3–5] In Ref. 1, highly (100) < uvw > oriented KTN(65/35) perovskite films were prepared from alkoxide precursors deposited on (100)$SrTiO_3$, and (100)MgO after annealing at 700, and 750 °C, respectively. In Ref. 3, highly (100) < uvw > oriented KTN(65/35) perovskite films were prepared from hydrolysed alkoxide sols deposited on (100)MgO and annealed at 700°C, only pyrochlore phase was observed in KTN(65/35) films deposited on (100)Si, (1-102)Al_2O_3 and (01-10)SiO_2. In Ref. 4, more substrate types were tested for KTN(65/35) film preparation, in addition to those mentioned above, also Pt-coated (111)Si, (100)YSZ, (110)$SrTiO_3$, and (012)$LaAlO_3$ were used. The authors concluded that the phase composition of the KTN thin films had a strong dependency on the crystal structure of the substrates, while other processing parameters (chemical additives to sol, annealing regimes) played smaller roles. Using substrates with both lattice parameters and symmetry of structure close to KTN ((100) and (110)$SrTiO_3$ (100)MgO), pure perovskite phase has been obtained. On substrates which exhibit lower degree of crystallographic matching [(100)YSZ, (1-102)Al_2O_3, (012)$LaAlO_3$] the KTN films contained a varying portions of pyrochlore phase impurity. On substrates without any structural similarity (amorphous SiO_2 and Pt-coated (111)Si) only the pyrochlore phase was observed. In Ref. 5, the structural, dielectric, and ferroelectric properties of

* Corresponding author. Tel.: +420-2-6617-2195; fax: 420-2-2094-1502.
E-mail address: bursik@iic.cas.cz (J. Buršík).

0955-2219/03/$ - see front matter © 2003 Elsevier Ltd. All rights reserved.
doi:10.1016/S0955-2219(03)00206-1

series of KTN thin films with compositions (65/35, 50/50, and 35/65), and deposited on bare and Pt-coated (100)MgO have been studied. Pure perovskite phase has been grown on both types of substrates at 700 °C with high degree of preferred (100) orientation. In summary, in all above-mentioned papers the maximum content of Ta in KTN films reached 65%, and preparation of pure perovskite phase was successful only in case when crystallographically similar single crystal substrate (i.e. $SrTiO_3$ or MgO) was used.

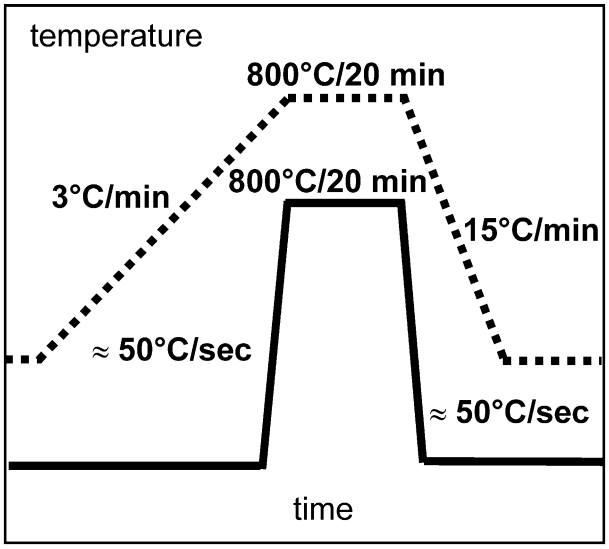

Fig. 1. Scheme of annealing procedures for thin KTN films: slow and fast heating regimes.

This paper describes the preparation of KTN perovskite thin films with high content of Ta ($\geqslant$95%) on either crystallographically similar [(100)MgO], or dissimilar [(100)Si, (0001)Al_2O_3, and SiO_2 glass] substrates using several types of buffer layers. These were chosen with respect to either their structural similarity with KT perovskite (KN, $PbTiO_3$, $PbTiO_3$–Al_2O_3 composite), or their chemical properties (Al_2O_3, YSZ). KTN films were successfully prepared after optimization of the following preparative factors: type and thickness of buffer layers, and heat-treatment conditions.

2. Experimental

$Ta(OCH_2CH(CH_3)_2)_5$, $Nb(OCH_2CH(CH_3)_2)_5$, and $K(OCH_2CH(CH_3)_2)$ were chosen as starting compounds for KT and KN sols, respectively, with absolute $HOCH_2CH(CH_3)_2$ as the solvent, and 2,2-diethanolamine as a modifier. The actual molar ratios of metals in KT and KN sols (to compensate potassium loss during heat treatment) were as follows: sol KT-A with

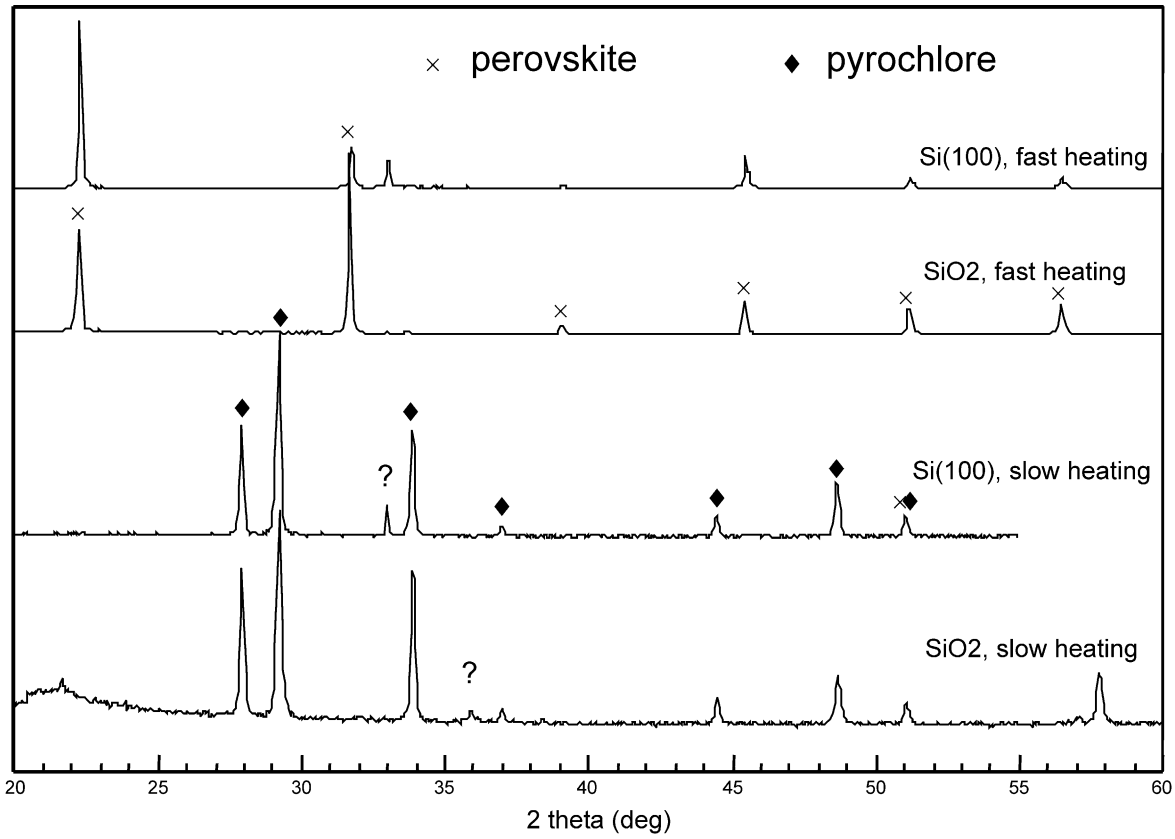

Fig. 2. XRD patterns of KTN films on SiO_2 and Si(100) substrates, with Al_2O_3 and KN buffer layers, pyrolysed at 600 °C for 5 min and annealed under slow and fast heating regimes.

K:Ta = 1.05, sol KT-B with K:Ta = 1.25, sol KN with K:Nb = 1.15. In order to minimize the loss of potassium, either through the evaporation or through the reaction with the underlaying layers, two types of KT sols were used. Potassium-enriched sol KT-B in the first and last deposition cycle, whereas sol KT-A for layers in between were used for deposition of KT layers. $Al(OCH_2CH(CH_3)_2)_5$ with absolute $HOCH_2CH(CH_3)_2$ as the solvent, and 2,2-diethanolamine as a modifier have been used for the preparation of sol for buffer layer deposition. Preparation of sols for deposition of other buffer layers [$PbTiO_3$, $PbTiO_3$–Al_2O_3 (Ti:Al = 2), YSZ (8% of Y)] are described in Ref. 6. The mixing of chemicals until the modifier was added was conducted in a dry nitrogen chamber, after that the solution of precursors was refluxed for 30 min, then modifier was added and solution was heated for several minutes. From this point the handling of solution was done in open atmosphere: unhydrolysed solutions were used for deposition by the spin–coating on SiO_2 glass, (100)MgO, (111)Si, (100)Si, (0001)Al_2O_3 substrates that were cleaned as described in Ref. 6. After the deposition the samples were dried (110 °C/3 min) in a drying chamber, then pyrolysed/crystallized in a preheated furnace for 5–10 min, and finally crystallized by annealing. When necessary the deposition/drying/pyrolysis cycle was repeated until the desired thickness was reached. Conditions for these pyrolyses and annealing steps differed in dependence on type of deposited layer. The Al_2O_3 buffer layer was pyrolysed at 450 °C for 5 min, and annealed at 900 °C for 15 min, YSZ and KN buffer layers were pyrolysed at 450 °C and annealed at 800 °C for 30 min, $PbTiO_3$, $PbTiO_3$–Al_2O_3 buffer layers were pyrolysed at 450 °C and annealed at 700 °C for 30 min. The KTN layers were pyrolysed at 600 °C and then annealed with different heating/cooling rates and annealing temperature/time periods in order to find optimum heat treatment conditions. The ultimate regimes (the slowest and fastest one) are depicted in the Fig. 1. For the first (slow) regime, the pyrolysed film was calcined at 800 °C for 20 min in air with the rate of heating and cooling 3, and 15 °C/min, from room to annealing temperature, respectively; while for the second (fast) one a procedure emulating the rapid thermal processing with the heating and cooling rates approximately to be 50 °C/s, was accepted. This second regime was realized by pushing of samples directly into the preheated furnace. To obtain the KT film of different thicknesses, the above procedure was repeated several times. The compositions of KTN sols and films were determined by means of the volumetric titration and electron microprobe analysis, respectively. The thickness

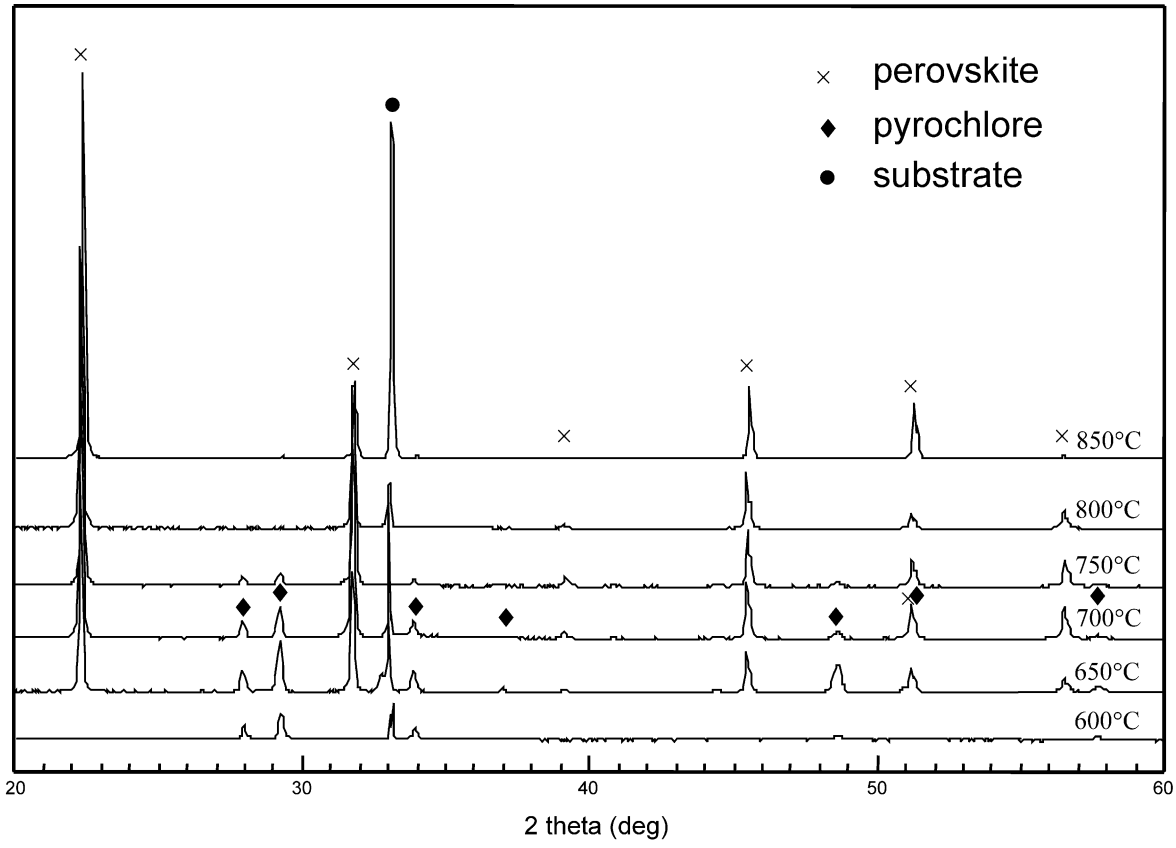

Fig. 3. XRD patterns of KTN films on SiO_2 glass substrate, with Al_2O_3 and KN buffer layers, heat-treated at different temperatures under fast heating regime.

of films was measured by the stylus profilometer, the crystallization behaviors of the CSD derived films were followed mainly by powder X-ray diffraction (XRD) and atomic force microscopy (AFM). To verify proofs about the perovskite structure gained by means of XRD, far infrared spectra were collected on selected samples.

3. Results and discussion

3.1. Heat-treatment regime

Fig. 2 shows XRD patterns of KTN films deposited on SiO_2 and Si(100) substrates, covered with Al_2O_3 and $KNbO_3$ buffer layers, pyrolysed at 600 °C for 5 min and annealed under slow and fast heating regimes at 800 °C for 20 min. Expressive difference in phase composition between these two ultimate annealing regimes can be observed: pure pyrochlore phase for slow, and pure perovskite phase for fast annealing. The result proves relevance of annealing mode used for this system. DTA/TG analysis of dried KT gels (not shown in this paper), exhibited gradual decrease in mass up to the temperature of 600 °C, where the sharp exothermic peak accompanied with abrupt mass decrease of 3–6% revealed. Taking into account the volatility and reactivity of potassium a strategy has been accepted to pyrolyse samples in a fastest way. Then potassium losses should be minimized by letting potassium to incorporate into crystalline structure. This was done by pushing as-deposited films into furnace preheated at 600 °C for 5 min. XRD patterns in Fig. 3 indicate that the pyrochlore phase crystallize at 600–650 °C and at higher temperatures (approx. 700 °C) starts to transform into the perovskite phase. At temperatures above 750 °C samples are formed by pure perovskite phase. This phase is stable up to approx. 850 °C, then the potassium deficient phase $K_6Ta_{10.9}O_{30}$ starts to reveal (not shown in the figure) and samples annealed above 900 °C are formed solely by this phase. These facts, together with those above mentioned, are indicative of crucial role which potassium content in the starting sols together with the fashion of annealing play in successful preparation of perovskite KT thin films. Too slow temperature ramp during annealing leads to slow pyrochlore to perovskite transformation and increased loss of potassium, perhaps both through the reaction with the substrate, and through evaporation into the atmosphere—even if the large over-supply of potassium relative to ideal KT stoichiometry is used. Further, there exists a temperature window between 750 and

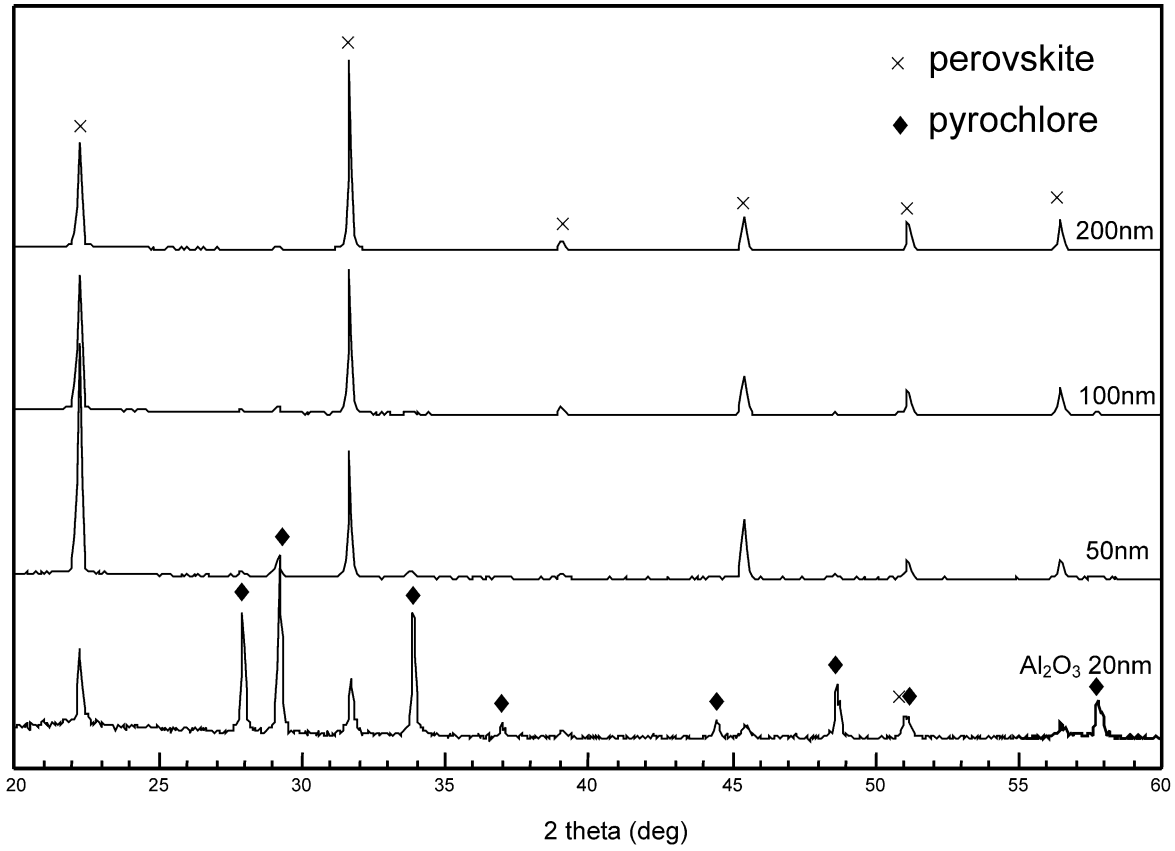

Fig. 4. XRD patterns of KTN films on (100)Si substrate with Al_2O_3 buffer layer of different thickness, and KN buffer layer (t 60 nm), annealed at 800 °C for 20 min under fast heating regime.

850 °C, in which the perovskite phase forms preferentially. Below the lower limit pyrochlore phase crystallizes preferentially, above the upper limit the formation of potassium deficit phases is inevitable.

3.2. Buffer layers

Taking into consideration the practical aspect of possible material expenses, the effort was made to develop procedure for preparation of KT perovskite using common and relatively cheap substrates. Though SiO_2 glass and (100)Si meet this demand, they exhibit acidic character. Then, the need of using buffer layers revealed oneself as a second key issue in solution of the problem how to avoid potassium losses. Using fast heating mode with annealing period 800 °C/20 min the effect of two buffer layers composed of Al_2O_3 or Y stabilized ZrO_2 was tested. Their role has been to separate potassium containing layers from acidic substrate (therefore designated here as "chemical" buffer layer). Whereas the efficiency of the latter in the crystallization of perovskite was not satisfactory (large roughness of buffer layer, crystallization of mixed phases), Al_2O_3 buffer layer exhibited both chemical inertness towards KN, KT phases, and very smooth surface (see also Fig. 6). As can be seen in the Fig. 4, below certain limit of Al_2O_3 film thickness (estimated to be about 200 nm) the samples are formed by mixture of pyrochlore and perovskite phases, whereas above this limit samples are constituted by pure perovskite phase. From this it can be concluded that Al_2O_3 film with thickness above 200 nm provides sufficient protection against excessive losses on potassium through reaction with acidic substrates. To promote further the successful crystallization of perovskite phase one more approach was examined—using a seeding layer. The effect of deposition of thin seeding layer for the growth of highly oriented polycrystalline films on substrates with dissimilar crystal structures and interatomic spacings using CSD method was described in Refs.[7–9]. Thus, in Ref. 7 it has been experimentally observed that thin films of ZrO_2 break into islands during grain growth. According to thermodynamic calculations done by authors this break-up lowers the free energy of the system when the grain-size-to-film-thickness ratio exceeds a critical value. This effect was used further in Refs. [8,9], where a two-step process was employed. In first step, thin seeding layer (YSZ in Ref. 8, or $PbTiO_3$ in Ref. 9) has been deposited and heat-treated to promote its break-up. This break-up favoured those grains that have a low substrate interfacial energy and so produced a film of highly oriented isolated grains. In the second step, remaining polycrystalline

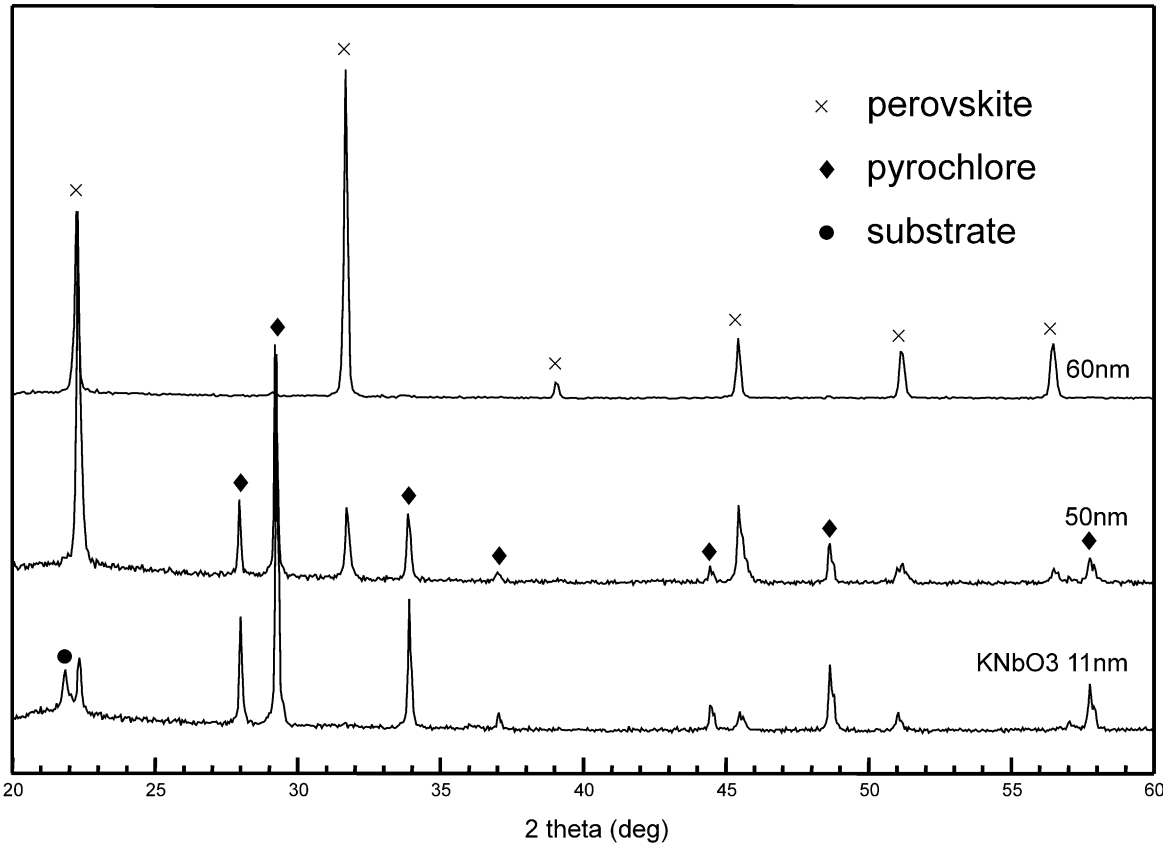

Fig. 5. XRD patterns of KTN films on (100)Si substrate with Al_2O_3 buffer layer ($t = 240$ nm) and KN buffer layer of different thickness, annealed at 800 °C for 20 min under fast heating regime.

films are deposited by CSD to produce a highly oriented film via grain growth from seed islands. Because KN exhibits lower melting point to KT (1039 and 1370 °C, respectively),[10] and because above 250 °C KN exhibits pseudocubic structure with lattice misfit of less then −2% towards $KTaO_3$ ($a=0.3996$, $c=4.063$ nm at 270 °C for KN, $a=4.0011$ nm for KT according to ICSD entries), the attempt was done to promote further the crystallization of KT perovskite phase using thin KN seeding layer. Fig. 5 illustrates the effect of thickness of KN seeding on phase composition of KTN films deposited on (100)Si substrate with Al_2O_3 buffer layer ($t=240$ nm), annealed at 800 °C for 20 min under fast heating regime. With increasing thickness of KN layer the portion of perovskite phase in the phase composition of KTN films increases. The thickness of KN seeding layer was estimated as 1/6 of the thickness of (for this purpose) six times deposited KN layer. With respect

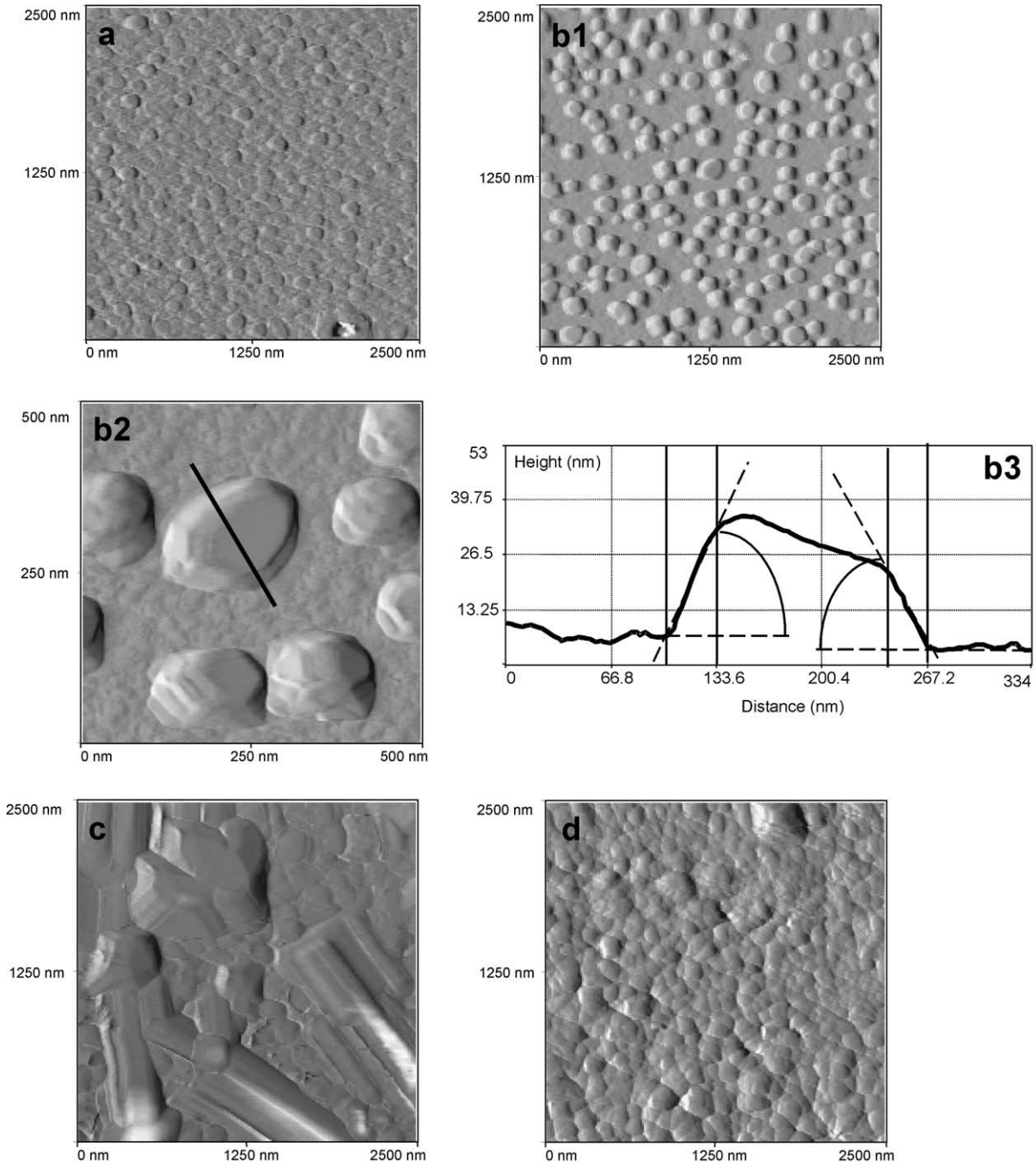

Fig. 6. AFM pictures of (a) Al_2O_3 buffer layer ($t=240$ nm) on Si(100), heat-treated at 900 °C for 1 h; (b1, b2, b3) and (c) KN buffer layer (equivalent thickness 50 nm and 60 nm, resp.) on the Si/Al_2O_3 substrate, heat-treated at 800 °C for 30 min; (d) KT film ($t=1200$ nm) on the Si/Al_2O_3/KN substrate, heat-treated at 800 °C for 20 min under fast heating regime.

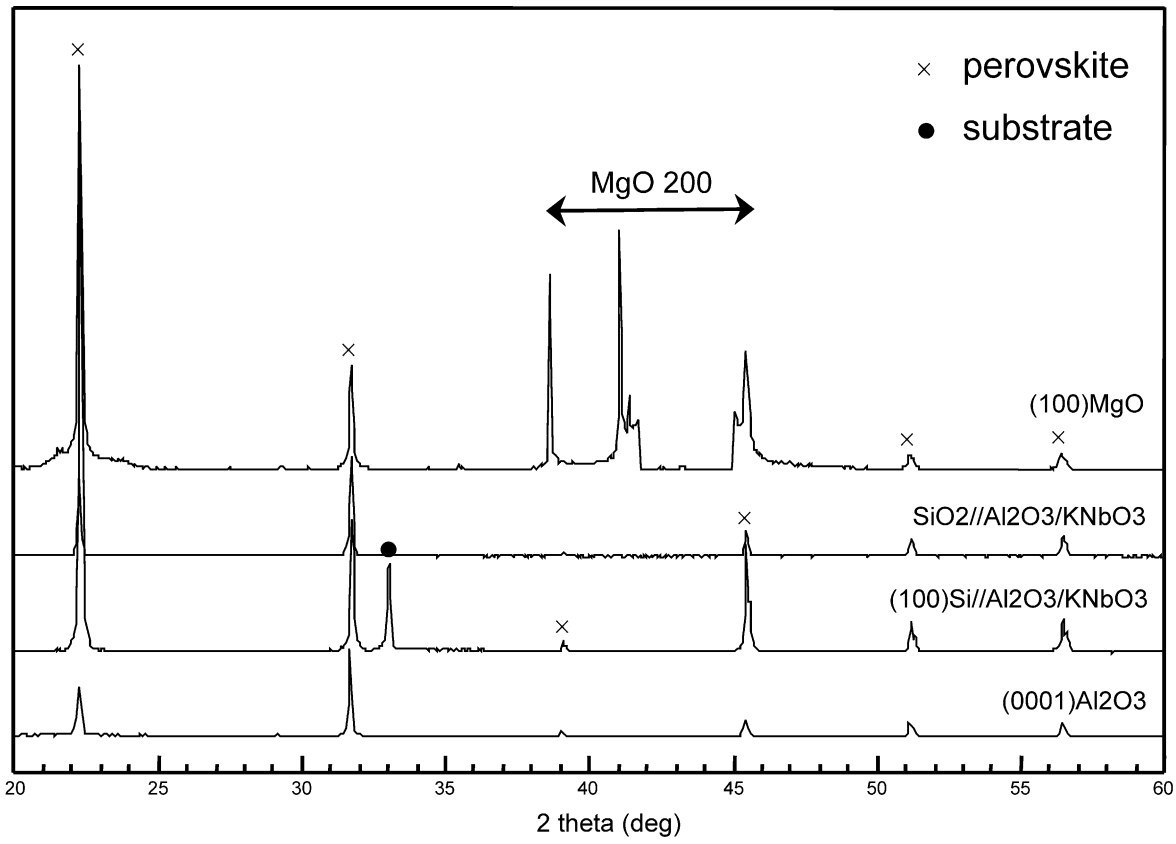

Fig. 7. XRD patterns of KTN films on different substrates, annealed at 800 °C for 20 min under fast heating regime.

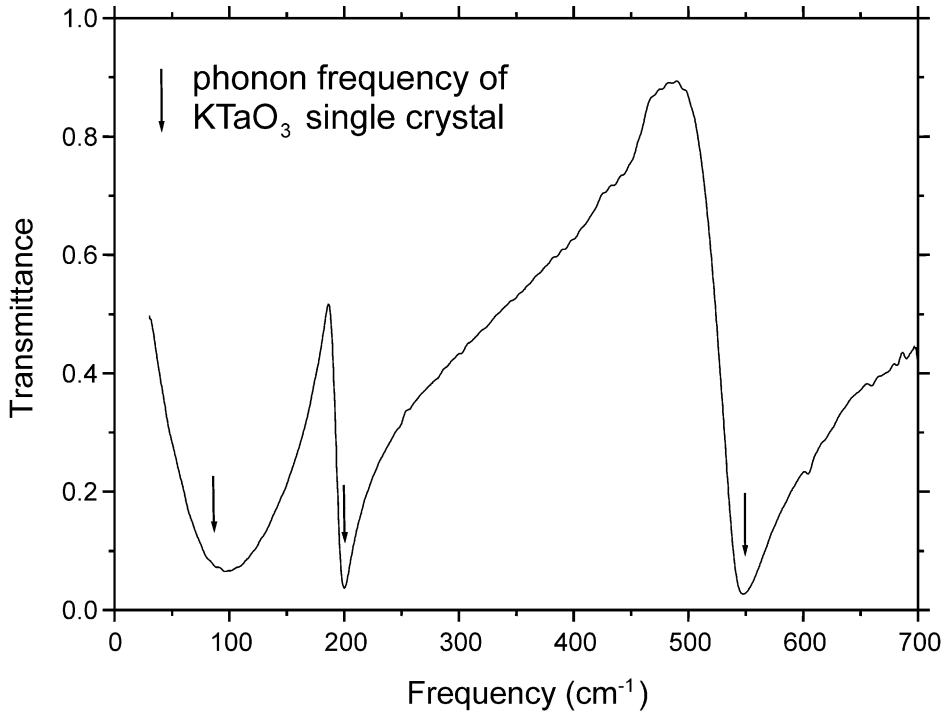

Fig. 8. Far infrared transmittance spectra on (100)Si/Al_2O_3/KN/KT thin film.

to high annealing temperature it is highly probable that pronounced interdiffusion of Nb and Ta occurred, forming a solid solution composition $KTa_{1-x}Nb_xO_3$. Simple balance calculation established on ratio of thicknesses of KN and KT layers (60 and 1200 nm, respectively) yields the x value in the summation formula to be 0.05. In fact, no Nb was detected in this KTN film by means of electron microprobe analysis. Fig. 6 shows AFM pictures of surface topography of gradually constituted layer stackings: (a) Al_2O_3 buffer layer on (100)Si heat-treated at 900 °C for 1 h; (b1, b2, and b3) and (c) KN buffer layers on Si covered with Al_2O_3 and heat-treated at 800 °C for 30 min; (d) KT film on the Si covered with Al_2O_3/KN buffer layers. The Al_2O_3 layer exhibits a compact and smooth surface (rms = 2.6) composed of fine grains which gave blank XRD pattern. Concerning KN seeding layer interesting phenomena was observed. The continuously covered surface of KN disintegrated itself into isolated islands which start to coalesce with increasing thickness of KN layer [compare Fig. 6(b1) and 6(c)]. Moreover, the walls of the grains exhibit features resembling facets of single crystals [see Fig. 6(b2) and profile cross-section of a KN grain in Fig. 6(b3)]. These features manifest itself also in increased roughness of surface (rms = 12.0), after deposition of the top KT layer [Fig. 6(d)] roughness decreased again with rms = 8.0. Thus, the breakup phenomenon seems to be of general nature and would deserve a greater attention in the future. Fig. 7 shows XRD patterns of KTN films deposited on different substrates. In all cases, the pure perovskite phase was obtained, surprisingly both on (0001)Al_2O_3, and on (100)MgO with only minor preferred orientation. To support proves about perovskite nature of KTN films, far infrared spectra were measured on series of KT/KN/Al_2O_3/Si(100) samples (Fig 8). The transmittance spectra are corrected in respect to substrate and Al_2O_3, KN buffer layers. The interference fringes coming from the substrate were removed by Fourier transform filtering. The three minima shown at 100, 200 and 550 cm^{-1} correspond to three optical active phonons in perovskite crystal structure. This provides clear proof of the perovskite structure of the film. For comparison, three arrows indicate the frequencies of these phonons measured on KT bulk single crystal.

Table 1
Phase composition of KTN thin films deposited on different substrates (and using different buffer layers) annealed under fast heating regimes, 800 °C for 20 min

Substrate	"Chemical" buffer layer	"Seeding" buffer layer	Composition of KTN layer[a]	Respective figures
SiO_2 glass	–	–	Py	
SiO_2 glass	Al_2O_3	–	Py + Pe	
SiO_2 glass	Al_2O_3	KN	Pe	2, 3, 7
SiO_2 glass	$PbTiO_3$	–	Py	
SiO_2 glass	$PbTiO_3$–Al_2O_3	–	Py + Pe (>10%)	
SiO_2 glass	YSZ	–	Py	
Si(100)	–	–	Py	
Si(100)	Al_2O_3	–	Pe + Py or Pe	4
Si(100)	Al_2O_3	KN	Pe	2, 5, 6d, 7, 8
Al_2O_3(0001)	–	KN	Pe	
Al_2O_3(0001)	–	–	Pe	7
MgO(100)	–	–	Pe	7

[a] pe, perovskite; py, pyrochlore.

4. Conclusions

A CSD method was used to form a polycrystalline film of $KTa_{1-x}Nb_xO_3$ with high content of Ta on different substrates (Table 1). For successful crystallization of perovskite phase on Si and SiO_2 substrates three factors are vital: potassium stoichiometry surplus, the ramp of annealing rate and presence of buffer layers.

Acknowledgements

This work was supported by the grants from The Ministry of Education of the Czech Rep. (LN00A028 and OC 528.001) and GACR (202/02/0238/A and 202/00/1245). Authors would also like to thank J. Chval, D. Chvostová and V. Studnička (IP ASCR) for EMPA, thickness and XRD measurements; P. Košovan and A. Petřina (IIC ASCR) for preparation of samples and XRD measurements, respectively.

References

1. Bao, D., Kuang, A. and Gu, H., *Phys. Stat. Sol. (a)*, 1997, **163**, 67.
2. Nakamura, K. and Imai, K. *Jpn. Kokai Tokkyo Koho* JP 08196328, 1996.
3. Hirano, S., Yogo, T., Kikuta, K., Morishita, T. and Ito, Y., *J. Am. Ceram. Soc.*, 1992, **75**, 1701.
4. Lu, C. J. and Kuang, A. X., *J. Mater. Sci.*, 1997, **32**, 4421.
5. Suzuki, K., Sakamoto, W., Yogo, T. and Hirano, S., *J. Am. Ceram. Soc.*, 1999, **82**, 1463.
6. Buršík, J., Kužel, R. and Vaněk, P., *Int. J. of Inorg. Mater.*, 2001, **3**, 485.
7. Miller, K. T., Lange, F. F. and Marshall, D. B., *J. Mater. Res.*, 1990, **5**, 151.
8. Miller, K. T. and Lange, F. F., *J. Mater. Res.*, 1991, **6**, 2387.
9. Kim, J. H. and Lange, F. F., *J. Mater. Res.*, 1999, **14**, 1626.
10. Reisman, A., Holtzberg, F., Berkenblit, M. and Berry, M., *J. Amer. Chem. Soc.*, 1956, **78**, 4517.